Coulomb-interaction-dependent effect of high-order sideband generation in an optomechanical system

Cui Kong, Hao Xiong, and Ying Wu

Phys. Rev. A **95**, 033820 — Published 20 March 2017

DOI: 10.1103/PhysRevA.95.033820

Coulomb-interaction dependent effect of high-order sideband generation in an optomechanical system

Cui Kong, Hao Xiong,* and Ying Wu†
School of Physics, Huazhong University of Science and Technology, Wuhan, 430074, P. R. China
(Dated: February 24, 2017)

High-order sideband generation in an optomechanical system coupled to a charged object is discussed, and the features of Coulomb-interaction dependent effect are identified. We show that the Coulomb-interaction dependent effect of high-order sideband generation exhibits essential difference between the case of weak control field and strong control field. In the weak control field case, the output spectra are in the perturbative regime and there is hardly any Coulomb-interaction dependent effect in an optomechanical system coupling to an object with a small amount of charge. In the strong control field case, the output spectra are in the nonperturbative regime and robust Coulomb-interaction dependent effect arises even if there are few charges. The amplitudes of specific sidebands are also discussed, and it is shown that Coulomb interaction plays an important role in achieving optomechanical control. Due to the extremely sensitive to charge number, Coulomb-interaction dependent effect of high-order sideband generation is remarkable in many aspects and may be used to precision measurement of electrical charges beyond the linearized optomechanical interaction.

PACS numbers: 03.65.Ta, 42.50.Wk

I. INTRODUCTION

Cavity optomechanics [1, 2], which treats resonantly enhanced feedback-backaction arising from radiation pressure, has become a rapidly developing research field recently and find applications in achieving high precision measurement [3] and on-chip manipulation of asymmetric light propagation [4, 5]. In general, an optomechanical system consists of a Fabry-Perot cavity in which one mirror of the cavity is movable as a mechanical resonator with angular frequency ω_m and mass m, and the optomechanical system is usually driven by a strong control field with frequency ω_1 and a weak probe field with frequency ω_p, especially in the setup of observing the signals of optomechanically induced transparency [6–8].

Optomechanically induced transparency, which enabled by radiation-pressure coupling of optical modes and mechanical oscillations [9, 10], is an interesting analog of electromagnetically induced transparency that originally discovered in atoms and molecules, and can be well understood through the linearization of the optomechanical interactions [11, 12]. In the parameter configuration of optomechanically induced transparency, ω_1 is detuned by about $-\omega_m$ from the cavity resonance frequency and the frequency difference between probe and control fields is chosen to be over the optical resonance of the cavity. Based on the linearized dynamics of the optomechanical interactions, a transmission window for the propagation of probe field is induced by the control field when the resonance condition is met. It has been shown that optomechanically induced transparency can be used to precisely measure the charge number of small charged objects due to the Coulomb-interaction dependent effect of the transmission window [13].

Recently, signals arising from the nonlinear optomechanical interactions have been revealed in both perturbative and non-perturbative regime and emerged as a new frontier in cavity optomechanics [2]. In the semiclassical mechanism, novel spectral components at the second- and higher-order sideband have been found based on the perturbative analysis [14] in the parameter configuration of optomechanically induced transparency. Full quantum calculations predict that the signal at the second order sideband exhibits a prominent feature of nonlinear optomechanically induced transparency [15]. These perturbative analysis provides a viable tool for inferring signals arising from the nonlinear optomechanical interactions with simple calculations. Based on the method, features of nonlinear optomechanical dynamics with multiple probe field driven have been discussed and sum and difference sideband generation [16] have been revealed, and typical spectral structure in the nonperturbative regime have been identified [17]. Recently, optomechanically induced sideband generation and chaos dynamics have been studied in various contents, including optomechanical system with second-order coupling [18], delaying or advancing higher-order sideband signals [19], hybrid electro-optomechanical systems [20, 21], photonic molecule optomechanical system [22], coherent-mechanical pumped optomechanical systems [23], and PT-symmetry optomechanics [24]. Analytical description of the intrinsic nonlinearity arising from quadratic optomechanical interactions [25] has also been discussed.

In the present work, we investigate the Coulomb-interaction dependent effect of high-order sideband generation in an optomechanical system coupled to a charged object and identify the features of Coulomb-interaction dependent effect. We find that the Coulomb-interaction dependent effect of high-order sideband generation exhibits essential difference between the case of weak control field and strong control field. In the weak control field case, the output spectra are in the perturbative regime and there is hardly any Coulomb-interaction dependent effect in an optomechanical system coupling to an object with a small amount of charge. In the strong control field case, the output spectra are in the nonperturbative regime and ro-

*Electronic address: haoxiong1217@gmail.com
†Electronic address: yingwu2@126.com

bust Coulomb-interaction dependent effect arises even if there are few charges. The Coulomb-interaction dependent effect of high-order sideband generation may be important in understanding the nonlinear optomechanical interactions and play an important role in achieving optomechanical control. From the precision measurement perspective, Coulomb-interaction dependent effect of high-order sideband generation may provide an potential method for precision measurement of electrical charge.

The paper is organized as follows. In Sec. II, we will present the theoretical model and give the derivation of Heisenberg-Langevin equation of motion. Linearized dynamics around the steady-state solution are introduced in brief in Sec. III. In Section IV, we show the features of Coulomb interaction-dependent effect in the perturbative regime, where typical spectral structure are discussed. In Section V, the features of Coulomb interaction-dependent effect of high-order sideband generation in the nonperturbative regime are shown. Finally, a conclusion of the results is summarized in Section VI.

II. THE THEORETICAL MODEL AND THE HEISENBERG-LANGEVIN EQUATION OF MOTION

As schematically shown in Fig.1, Coulomb interaction can be introduced to a conventional optomechanical system where a Fabry-Perot cavity consists of a fixed mirror and a movable one which treats as a mechanical resonator (MR). The Hamiltonian formulation of such a optomechanical system reads [13, 26]:

$$\hat{H}_0 = \hbar\omega_c \hat{a}^\dagger \hat{a} + (\frac{\hat{p}^2}{2m} + \frac{m\omega_m^2 \hat{x}^2}{2}) + \hbar G \hat{x}\hat{a}^\dagger \hat{a} + \frac{kQ_1Q_2}{r-\hat{x}}, \quad (1)$$

where the first term $\hbar\omega_c \hat{a}^\dagger \hat{a}$ is the free Hamiltonian of the cavity, in which $\hat{a}^\dagger$ ($\hat{a}$) is bosonic creation (annihilation) operator of the single-mode cavity with eigenfrequency ω_c. The second term $\hat{p}$ and $\hat{x}$ are the momentum and position operators of the movable mirror with effective mass m and angular frequency ω_m. The third term denotes the coupling between the cavity field and the movable mirror via radiation pressure with the coupling strength G. The last term presents the interaction of the charged MR with the charged body by a Coulomb force, where k is the electrostatic force constant, r is the distance between the MR and the charged body, and Q_1 and Q_2 are the charge of MR and the charged body, respectively. For simplicity, in the present work we only focus on the case that the direction of the Coulomb force on the MR is the same as the radiation pressure, and a possible choice is $Q_1 > 0$ while $Q_2 = ne < 0$ with n the charge number.

Let us now assume that a strong driving field and a weak-probe field, with frequencies ω_1 and ω_p, respectively, are applied to the cavity. Then the Hamiltonian of the optomechanical system can be written as:

$$\hat{H} = \hat{H}_0 + i\hbar\left[\left(\varepsilon_1 e^{-i\omega_1 t} + \varepsilon_p e^{-i\omega_p t}\right)\hat{a}^\dagger - \text{H.c.}\right]. \quad (2)$$

The amplitudes of the pump field and the probe field are defined as $\varepsilon_1 = \sqrt{P_1/\hbar\omega_1}$ with the pumping field's power P_1 and $\varepsilon_p = \sqrt{P_p/\hbar\omega_p}$ with the probe field's power P_p, where the amplitudes of the pump field and the probe field are normalized to a photon flux at the input of the cavity.

Considering about $\langle\hat{x}\rangle \ll r$, we make use of series expansion, so $kQ_1Q_2/(r-\hat{x})$ can be written as $kQ_1Q_2\hat{x}/r^2$, where higher order terms of $\hat{x}$ is omitted. Therefore the total Hamiltonian can be described as follows [13]:

$$\begin{aligned}\hat{H} =& \hbar\omega_c \hat{a}^\dagger \hat{a} + \frac{\hat{p}^2}{2m} + \frac{m\omega_m^2 \hat{x}^2}{2} + \hbar G \hat{x}\hat{a}^\dagger \hat{a} + \frac{kQ_1Q_2\hat{x}}{r^2} \\ &+ i\hbar\left[\left(\varepsilon_1 e^{-i\omega_1 t} + \varepsilon_p e^{-i\omega_p t}\right)\hat{a}^\dagger - \text{H.c.}\right]. \end{aligned} \quad (3)$$

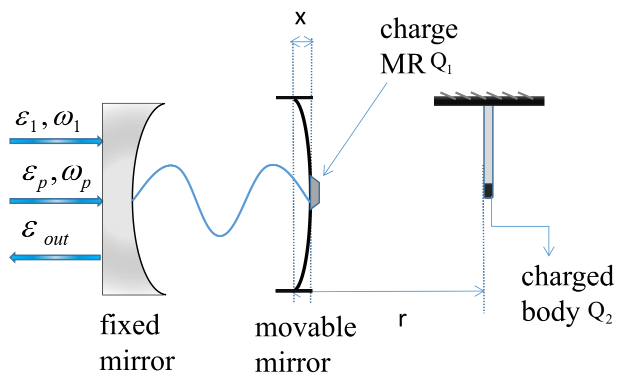

FIG. 1: Schematic diagram of an optomechanical system where the MR is charge coupling to an adjoining charged body. The optomechanical system is driven by a strong pump field with frequency ω_1 and the weak probe field with frequency ω_p. The output field is represented by ε_{out}. Through the control of the strength of the driving field and the charge, we can get different features of the output high-order sidebands spectrum.

Transforming the Hamiltonian Eq.(3) into the rotating frame at the frequency ω_1 of the input laser based on $\hat{H}_1 = \hbar\omega_1\hat{a}^\dagger\hat{a}$, $U_t = e^{-i\hat{H}_1 t/\hbar} = e^{-i\omega_1\hat{a}^\dagger\hat{a}t}$, and $\hat{H}_{rot} = U^\dagger(\hat{H} - \hat{H}_1)U$, the resulting effective Hamiltonian can be derived as:

$$\begin{aligned}\hat{H}_{\text{eff}} =& \hbar\Delta_c \hat{a}^\dagger \hat{a} + \frac{\hat{p}^2}{2m} + \frac{m\omega_m^2 \hat{x}^2}{2} + \hbar G \hat{x}\hat{a}^\dagger \hat{a} + \frac{kQ_1 ne\hat{x}}{r^2} \\ &+ i\hbar\left[\left(\varepsilon_1 + \varepsilon_p e^{-i\delta t}\right)\hat{a}^\dagger - \text{H.c.}\right], \end{aligned} \quad (4)$$

where $\Delta_c = \omega_c - \omega_1$ is the detuning of the input control field from the cavity resonance frequency and $\delta = \omega_p - \omega_1$ is the detuning between the frequency of the probe field and the control field. Based on the effective Hamiltonian and introducing the dissipation and fluctuation terms by using the Markov approximation, the Heisenberg-Langevin equation of motion can be written as:

$$\begin{aligned}\dot{\hat{x}} =& \frac{\hat{p}}{m}, \\ \dot{\hat{p}} =& -m\omega_m^2\hat{x} - \frac{kQ_1 ne}{r^2} + \hbar G\hat{a}^\dagger\hat{a} - \gamma_m\hat{p} + \hat{F}_{th}, \\ \dot{\hat{a}} =& -\left[\kappa + i\left(\Delta_c + G\hat{x}\right)\right]\hat{a} + \left(\varepsilon_1 + \varepsilon_p e^{-i\delta t}\right) + \hat{a}_{in}, \end{aligned} \quad (5)$$

where κ is the loss rate of the cavity and γ_m is the mechanical decay rate introduced classically. $\hat{F}_{th}$ and $\hat{a}_{in}$ denote environmental noises corresponding to the operators $\hat{p}$ and $\hat{a}$, respectively. In this work, we are interested in the mean response of the system, so the operators can be reduced to their expectation values. Thus the evolution of the optomechanical system can be described by the following equations:

$$\begin{aligned}\dot{x} =& \frac{p}{m},\\ \dot{p} =& -m\omega_m^2 x - \frac{kQ_1 ne}{r^2} + \hbar G a^* a - \gamma_m p,\\ \dot{a} =& -[\kappa + i(\Delta_c + Gx)]\, a + \varepsilon_1 + \varepsilon_p e^{-i\delta t},\end{aligned} \tag{6}$$

where the quantum noise terms are safely ignored in the weak-optomechanical coupling regime [1].

III. DYNAMICS AROUND THE STEADY-STATE SOLUTION

Equations (6) are nonlinear and coupled equations due to the parametric coupling between the optical and mechanical modes. The steady-state solution of Eqs. (6) can be obtained as

$$a_s = \frac{\varepsilon_1}{\kappa + i\Delta}, \quad x_s = \frac{\hbar G a_s^2 - kQ_1 ne/r^2}{m\omega_m^2}, \tag{7}$$

with $\Delta = \Delta_c - Gx$. Equations (7) give functions mapping the intracavity photon number $|\bar{a}|^2$ to the displacement $\bar{x}$ under different Coulomb interactions. This system has bistability if the control field is strong enough. Coupled equations with multiple steady states have also been found in nonlinear optics [27] and economic evolution [28], and lead to complex dynamics. Figure 2 shows the displacement x_s varies with the power of the control field and charge number by solving Eqs. (7) numerically. All the parametric values are adopted from the experiment [13]: $\lambda_c \equiv 2\pi c/\omega_c$ =1046 nm, $G/2\pi = -11$ MHz/nm, $m = 145$ ng, $\kappa = 2\pi \times 215$ kHz, $\omega_m = 2\pi \times 947$ kHz, $\gamma_m = 2\pi \times 141$ Hz, $r = 67\mu$m, $\varepsilon_1 = \sqrt{2P_1\kappa/\hbar\omega_c}$ and $Q_1 = CU$, $C = 27.5$ nF, with $U = 1$ V. From Fig. 2, It is obvious to find that both the power of the control field and charge number have an influence on the displacement x_s of the MR and the effect is positive. This phenomenon can be easily explained by the fact that the MR is subjected to the radiation pressure and Coulomb force with the same direction, and the displacement x_s enlarges with the enhancement of both the power of the control field and charge number.

If the probe field is much weaker than the control field, dynamics around the steady-state solution can be analyzed perturbatively. The control field provides the system with a steady-state, the dynamics of intracavity field driven by the probe field can be served as the perturbation or noise of the steady state. The solution of Eqs. (6) can be written as

$$x = x_s + \delta_x, \quad a = a_s + \delta_a, \tag{8}$$

where δ_a and δ_x are the fluctuations of cavity field and the displacement of the MR around the steady-state solution, respectively. Substituting solution (8) into Eqs. (6), we can obtain a group of differential equations with the nonlinear terms

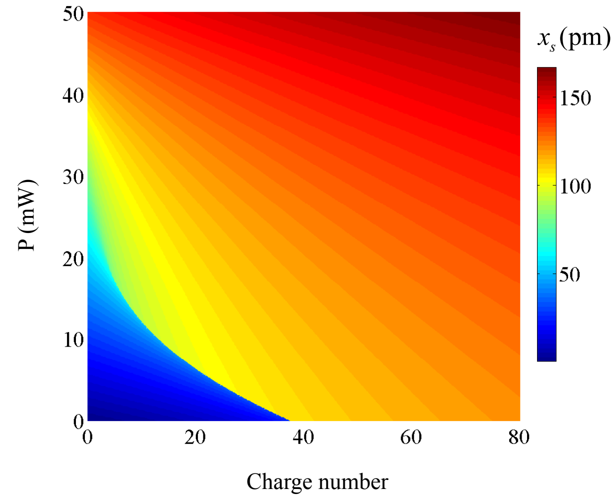

FIG. 2: The displacement x_s as function of the power of the control field and charge number. The parameters are $\Delta_c = \omega_m = \delta$, $\lambda_c \equiv 2\pi c/\omega_c = 1064$ nm, $G/2\pi = -11$ MHz/nm, $m = 145$ ng, $\kappa/2\pi = 215$ kHz, $\omega_m/2\pi = 947$ kHz, $\gamma_m/2\pi = 141$ Hz, $r = 67\mu$m, and $Q_1 = CU$ with $C = 27.5$ nF and $U = 1$ V [13].

$-iG\delta x\delta a$ and $\hbar G\delta a^*\delta a/m$. Ignoring these nonlinear terms leads to the linearization of dynamic equations, which can be solved by using the following ansatz:

$$\delta_x = A^- e^{-i\delta t} + A^+ e^{i\delta t}, \quad \delta_a = C^- e^{-i\delta t} + C^+ e^{i\delta t}, \tag{9}$$

where $(A^-)^* = A^+$ due to the real nature of the displacement of the MR. By making use of the input-output relation, the output field S_{out} of the optomechanical system can be obtained. This linearized evolution can be described as the Stokes processes with frequencies $\omega_1 - \delta = 2\omega_1 - \omega_p$ and the anti-Stokes processes with frequencies $\omega_1 + \delta = \omega_p$. When the resonance frequency of the movable mirror is equal to the resonance condition of the cavity, the Stoke field is strongly suppressed and the anti-Stoke field is resonantly enhanced, so the probe field is coherent with the anti-Stokes sideband, leading to an adjustable transparency window, which is the phenomenon of optomechanical induced transparency (OMIT). The linearization of equations (6), which corresponding to linearized dynamics of the optomechanical system with a mechanical driving, are studied in Ref. [10, 11], where optomechanically induced transparency and slow light have been discussed.

IV. COULOMB INTERACTION-DEPENDENT EFFECT OF TYPICAL SPECTRAL STRUCTURE IN THE PERTURBATIVE REGIME

The linearization of dynamic equations is usually used to describe optomechanically induced transparency. To discuss nonlinear optomechanical interactions, the nonlinearity of these equations must be taken account. It has been predicted that, if taking into account the nonlinear terms $-iG\delta x\delta a$ and $\hbar G\delta a^*\delta a/m$, there are output fields at frequencies $\omega_1 \pm j\delta$

generation, with j an integer that express the order of the sidebands [14]. There are two kinds of feature of the high-order sideband generation spectra: one is perturbative signs in the spectral structure, where only several order sidebands can be seen and the amplitude of the higher-order sidebands scale perturbatively with the strength of the drive laser; The other appear more robust and reveals the nonperturbative regime of the optomechanical interaction. For high-order sideband generation in the perturbative regime, the amplitude of higher order sideband is smaller and each order of sidebands reduces the amplitude sharply. For high-order sideband generation in the nonperturbative regime, it decreases rapidly for the first few order sidebands, followed by a plateau where all the sidebands have the same strength, and ends up with a sharp cutoff [17]. Different from the optomechanically induced transparency in the linearized dynamics, the amplitudes of high-order sideband generation are quite difficult to obtain analytically.

In the present work, the evolution equations (6) are solved numerically without taking into account the weak probe field approximation. The output spectrum $S(\omega) \propto |\int_{-\infty}^{\infty} s_{out}(t)e^{-i\omega t}dt|$ can be obtained by performing fast Fourier transform of $s_{out}(t)$, and high-order sideband generation with typical spectral structure is demonstrated numerically. We observe a Coulomb-interaction dependent effect of high-order sideband generation in the optomechanical system where different features of high-order sidebands spectrum generated with various charge numbers. We show that such Coulomb-interaction dependent effect reflects in two aspects: typical spectral structure and the amplitudes of specific sidebands. Coulomb-interaction dependent effect for the typical spectral structure becomes evident in the perturbative regime only when the charge number is big enough, while Coulomb-interaction dependent effect for the amplitudes of specific sidebands become obvious in the nonperturbative regime even if the charge number is quite small.

Figure 3 shows frequency spectra output from the optomechanical system with different charge number when the power of the control field is relatively weak (here we choose 10 mW for example). In Fig. 3(a), the value of charge number n is 0 and just a few order sidebands can be created, the maximum order is about 3. We can see clearly that the output spectra is in the perturbative regime, although there are second and higher order sideband components. The higher order of sideband is, the weaker the intensity of the high-order sideband is, which is presented by a linear decreasing perturbation trend. In Fig. 3(b), the charge number n increase to 10. It seems that Fig. 3(a) and Fig. 3(b) are almost the same, regardless of the order of the sideband or the strength of the sideband. Based on the comparison of the above two figures, we may safely draw the conclusion that under the condition of weak control field, there is hardly any Coulomb-interaction dependent effect of high-order sideband generation in an optomechanical system coupling to an object with a small amount of charge.

In order to observe Coulomb-interaction dependent effect of high-order sideband generation in the optomechanical system, we continue to increase the charge number of charged objects to 33, and the frequency spectra output from the optomechanical system is shown in Fig. 3(c), from which we find that some non-perturbative signs arise in the spectral structure. For example, the amplitude of the second-order sideband is nearly equal to the amplitude of the first-order sideband, which breaks the characteristic of perturbation. We also note that both the order and the intensity of high-order sidebands are increased relative to the Fig. 3(b). However, on the whole, the intensity of the sidebands decays along with the increase of sideband order, particularly for the third and higher order sidebands.

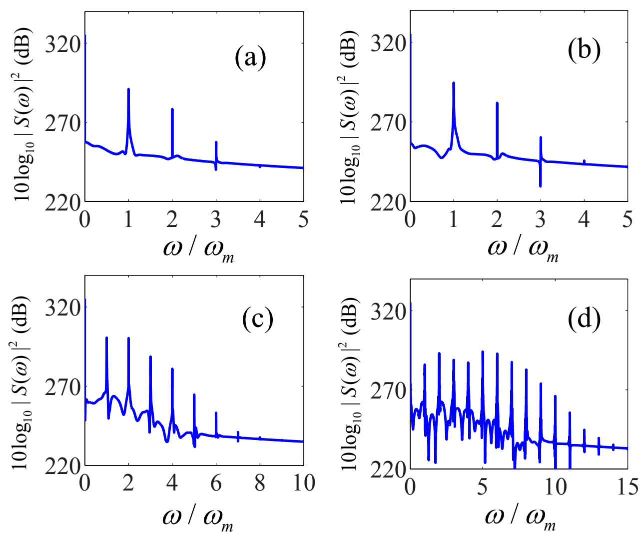

FIG. 3: Frequency spectra output from the optomechanical system is shown with various charge number. The frequency spectra output shift a frequency ω_1 due to the evolution of the cavity field in a frame rotating at the frequency ω_1. We use $\varepsilon_p = \varepsilon_1/2$. The power of the control field is $P_1 = 10$ mW and the charge number vary from 0, 10, 33 to 80 in (a),(b),(c),(d) respectively.

To get a much clear non-perturbative sign, we increase the amount of charge number to 80, and the frequency spectra output from the optomechanical system are shown in Fig. 3(d). The intensity of the high-order sidebands decreases rapidly for the first few order sidebands, followed by a plateau where all the sidebands have almost the same strength, and ends up with a sharp cutoff at the order of about 8, which distinctly shows that the high-order sideband spectrum is in the non-perturbative regime.

From the above discussion, we can summarize that only the charge number is big enough, can the Coulomb-interaction dependent effect of high-order sideband generation in an optomechanical system achieve when the power of the control field is weak. As a matter of fact, this phenomenon can be well explained by the nonlinear optomechanical interaction, in which the magnitude of the Coulomb force directly determines the magnitude of the mechanical displacement. Compared to traditional enhancement of high-order sideband generation by increasing the power of the driving field, Coulomb-interaction dependent effect in an optomechanical system coupling to charge object provides another way for the control of high-order sideband generation.

It is worthy of note that the results shown in Fig. 3 have not any contradiction to the typical feature of optomechanically induced transparency, which has a wide Lorentzian dip (describing the optical cavity mode) with a sharp transparency window at detuning ω_m from the control field frequency ω_1. In a typical spectrum of optomechanically induced transparency, the x-axis is δ which describes the detuning between the frequency of the probe field and the control field. For a fixed δ, only a transmissivity of the probe field can be obtained, which also are related to the amplitude of the first-order sideband. We must vary δ (usually, the probe field with wide spectrum may be used) to observe the effect of optomechanically induced transparency: a wide Lorentzian dip with a sharp transparency window. In the present work, both probe and control fields are monochromatic, and δ is fixed to be ω_m, thus such feature can not be observed in any of the spectra. To observe and analyze the typical optomechanically induced transparency feature in higher-order sideband generation, We should vary δ and discuss the amplitudes of the specific sidebands. In fact, some previous works have been done on this topic, and an inverted optomechanically induced transparency feature is found for the amplitude of the second order sideband [14].

V. COULOMB INTERACTION-DEPENDENT EFFECT OF HIGH-ORDER SIDEBAND GENERATION IN THE NONPERTURBATIVE REGIME

In this Section, we discuss Coulomb interaction-dependent effect of high-order sideband generation in the nonperturbative regime. Spectral structure of output fields from the optomechanical system is shown in Fig. 4(a), where the value of charge number n is 0 and the power of the control field is 20 mW. Unlike the perturbative spectral structure of output fields shown in Fig. 3(a), the amplitude of the second-order sideband is larger than the amplitude of the first-order sideband, which confirms the characteristic of non-perturbative signs. From Fig. 4(a) we observe that the cutoff order is about 4, thus we focus on the amplitudes of these specific sidebands.

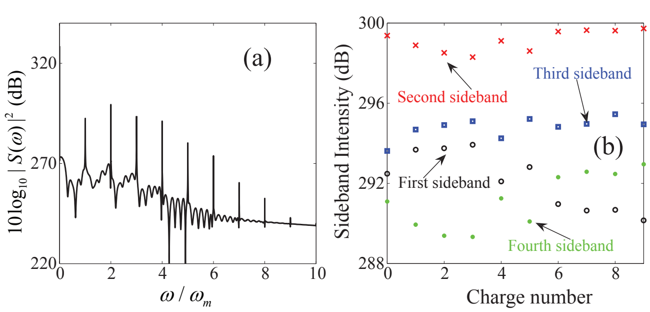

FIG. 4: (a) Frequency spectra output from the optomechanical system without Coulomb force. (b) The amplitudes of high-order sideband generation with different charge number from 0 to 9. The power of the control field is 20 mW and we use $\varepsilon_p = \varepsilon_1/2$.

Figure 4(b) shows the amplitudes of four different sidebands vary with charge number (from 0 to 9) when the power of the control field is 20 mW. All sidebands exhibit certain Coulomb interaction-dependent effect which, however, are not monotone increasing. The modification of the amplitudes of these four sidebands can achieve as large as 3 dB, which implies that the charge number have a notable impact on the sideband intensity. In particular, we observe that a single charge is enough to produce numerical difference about 1.5 dB, which can be easily detected by the current level of technology [29, 30] and makes possible a measurement of the charge number in high precision.

From the above discussion in the nonperturbative regime, we show that there are Coulomb-interaction dependent effects of high-order sideband generation in an optomechanical system even if the charge number is quite small. Due to the extreme sensitivity to charge number, Coulomb-interaction dependent effect of high-order sideband generation should work well even for detecting single charge in very small objects, and our scheme, which take advantage of nonlinear optomechanical interaction, may play an important role in achieving optomechanical control beyond the scheme based on the linearized optomechanical interaction.

We note that the sideband intensities do not show a monotonic trend for different charge numbers in Fig. 4(b), which brings difficulty for the determination of the charge number based on the intensity of a single sideband. There are two methods to overcome this difficulty: one method is to find a monotonic trend of sideband intensities on the charge number via adjusting the parameters of the system; the another is using the intensities of multiple sidebands. Although one can find a monotonic trend of sideband intensities on the charge number via adjusting the parameters of the system, the first method may be restricted by the real experiment condition and thus is not convenient to practical application. For the second method, we can determine the charge number via comparing the intensities of multiple sidebands, which is quite similar to the determination of carrier-envelope phase in an optical pulse with few cycles. Fortunately, the charge number is not large and the method is effective. For the case that the charge number is larger than 20, the present method is ineffective and in this case one may refer to the perturbative regime where modification of typical spectral structure is shown in Fig. 3 when the charge number is large.

VI. CONCLUSIONS

In summary, we investigate the Coulomb-interaction dependent effect of high-order sideband generation in an optomechanical system coupled to a charged object, and find that the Coulomb-interaction dependent effect of high-order sideband generation exhibits essential difference between the case of weak control field and strong control field. In the weak control field case, the output spectra are in the perturbative regime and there is hardly any Coulomb-interaction dependent effect in an optomechanical system coupling to an object with a small amount of charge. In the strong control field case, the output spectra are in the nonperturbative regime and robust Coulomb-interaction dependent effect arises even if there are few charges. The amplitudes of specific sidebands are also discussed, and it is shown that Coulomb interaction plays an important role in achieving optomechanical control. From the precision measurement perspective, Coulomb-interaction dependent effect of high-order sideband generation may provide an potential method for precision measurement of electrical charge.

Acknowledgments

The work was supported by the National Science Foundation of China (Grant Nos. 11405061, 11375067, and 11574104) and the National Key Research and Development Program of China (Grant No. 2016YFA0301203).

[1] M. Aspelmeyer, T. J. Kippenberg, and F. Marquardt, Cavity optomechanics, Rev. Mod. Phys. **86,** 1391 (2014).

[2] H. Xiong, L. Si, X. Lü, X. Yang, and Y. Wu, Review of cavity optomechanics in the weak-coupling regime: from linearization to intrinsic nonlinear interactions, Science China Physics, Mechanics & Astronomy, **58,** 050302 (2015).

[3] W. He, J. J. Li, and K. D. Zhu, Coupling-rate determination based on radiation-pressure-induced normal mode splitting in cavity optomechanical systems, Opt. lett. **35**, 339 (2010).

[4] H. Xiong, L.-G. Si, X. Yang, and Y. Wu, Asymmetric optical transmission in an optomechanical array, Appl. Phys. Lett. **107**, 091116 (2015).

[5] X.-W. Xu and Y. Li, Optical nonreciprocity and optomechanical circulator in three-mode optomechanical systems, Phys. Rev. A **91,** 053854 (2015).

[6] S. Weis, et al., Optomechanically Induced Transparency, Science **330**, 1520 (2010).

[7] F. Lei, et al., Dynamic Fano-like resonances in erbium-doped whispering-gallery-mode microresonators, Appl. Phys. Lett. **105**, 101112 (2014).

[8] H. Xiong, Y. M. Huang, L. L. Wan, Y. Wu, Vector cavity optomechanics in the parameter configuration of optomechanically induced transparency, Phys. Rev. A **94**, 013816 (2016); H. Xiong, C. Kong, X. Yang, Y. Wu, Optical polarizer based on the mechanical effect of light, Opt. lett. **41**(18), 4316-4319 (2016).

[9] B. P. Hou, L. F. Wei, and S. J. Wang, Optomechanically induced transparency and absorption in hybridized optomechanical systems, Phys. Rev. A **92**, 033829 (2015).

[10] Q. Wu, J. Q. Zhang, J. H. Wu, M. Feng, Z. M. Zhang, Tunable multi-channel inverse optomechanically induced transparency and its applications, Opt. Express **23**, 18534 (2015).

[11] P. C. Ma, J. Q. Zhang, Y. Xiao, M. Feng, and Z. M. Zhang, Tunable double optomechanically induced transparency in an optomechanical system, Phys. Rev. A **90**, 043825 (2014); E. Wu, F. Z. Li, X. F. Zhang, and Y. H. Ma, Optomechanical entanglement of a macroscopic oscillator by quantum feedback, International Journal of Quantum Information **14**, 1650022 (2016).

[12] C. Jiang, H. Liu, Y. Cui, X. Li, G. Chen, and B. Chen, Electromagnetically induced transparency and slow light in two-mode optomechanics, Optics Express **21**, 12165–12173 (2013).

[13] J.-Q. Zhang, Y. Li, M. Feng, Y. Xu, Precision measurement of electrical charge with optomechanically induced transparency, Phys. Rev. A **86,** 053806 (2012).

[14] H. Xiong, L.-G. Si, A.-S. Zheng, X. Yang, and Y. Wu, Higher-order sidebands in optomechanically induced transparency, Phys. Rev. A **86,** 013815 (2012).

[15] K. Børkje, A. Nunnenkamp, J. D. Teufel, and S. M. Girvin, Signatures of Nonlinear Cavity Optomechanics in the Weak Coupling Regime, Phys. Rev. Lett. **111,** 053603 (2013).

[16] H. Xiong, L.-G. Si, X.-Y. Lü, and Y. Wu, Optomechanically induced sum sideband generation, Opt. Express **24**, 5773-5783 (2016); H. Xiong, Y.-W. Fan, X. Yang, and Y. Wu, Radiation pressure induced difference-sideband generation beyond linearized description, Appl. Phys. Lett. **109**, 061108 (2016).

[17] H. Xiong, L.-G. Si, X.-Y. Lü, X. Yang, and Y. Wu, Carrier-envelope phase-dependent effect of high-order sideband generation in ultrafast driven optomechanical system, Opt. Lett. **38**, 353 (2013); Nanosecond-pulse-controlled higher-order sideband comb in a GaAs optomechanical disk resonator in the non-perturbative regime, Annals of Physics **349**, 43 (2014).

[18] C. Wang, H. J. Chen, K. D. Zhu, Nonlinear optical response of cavity optomechanical system with second-order coupling , Applied Optics **54**, 4623 (2015).

[19] Y. Jiao, H. Lü, J. Qian, Y. Li, and H. Jing, Nonlinear optomechanics with gain and loss: amplifying higher-order sideband and group delay, New Journal of Physics, **18**(8), 083034 (2016).

[20] B. Chen, L. D. Wang, J. Zhang, A. P. Zhai, and H. B. Xue, Second-order sideband effects mediated by microwave in hybrid electro-optomechanical systems, Phys. Lett. A, **380,** 798-802 (2016).

[21] M. Wang, et al., Controllable chaos in hybrid electro-optomechanical systems, Scientific Reports **6,** 22705 (2016).

[22] C. Cao, et al., Tunable high-order sideband spectra generation using a photonic molecule optomechanical system, Scientific Reports **6,** 22920 (2016).

[23] J. Ma, et al., Optomechanically induced transparency in the presence of an external time-harmonic-driving force, Scientific Reports **5,** 11278 (2015).

[24] X.-Y. Lü, H. Jing, J. Ma, and Y. Wu, P-T symmetry breaking chaos in optomechanics, Phys. Rev. Lett. **114,** 253601 (2015).

[25] S. Khorasani, Analytical solution of nonlinear optomechanics, arXiv:1702.04982 (2017).

[26] C. K. Law, Interaction between a moving mirror and radiation pressure: A Hamiltonian formulation, Phys. Rev. A **51**, 2537 (1995).

[27] H. Xiong, L.-G. Si, C. Ding, X. Y. Lü, X. Yang, and Y. Wu, Solutions of the cylindrical nonlinear Maxwell equations, Phys. Rev. E **85,** 016602 (2012).

[28] Y. Shi and M. Pan, Evolutionary dynamics of social tolerance in the economic interaction model with local social cost functions, Appl. Econ. Lett. **24,** 75-79 (2017).

[29] A. H. Safavi-Naeini, et al., Electromagnetically induced transparency and slow light with optomechanics, Nature **472**, 69 (2011).

[30] W.-X. Yang, High-order harmonics in a quantum dot and metallic nanorod complex, Opt. Lett. **40**, 4903 (2015).